GEOPHYSICS, VOL. 81, NO. 3 (MAY-JUNE 2016); P. P23–P31, 11 FIGS.
10.1190/GEO2015-0271.1

CrossMark
click for updates

Downloaded 08/03/16 to 131.180.58.123. Redistribution subject to SEG license or copyright; see Terms of Use at http://library.seg.org/

On the mechanical vibrator-earth contact geometry and its dynamics

Rik Noorlandt[1] and Guy Drijkoningen[2]

ABSTRACT

The geometry of the contact between a vibrator and the earth underneath influences the dynamics of the vibrator. Although a vibrator might appear to be well-coupled with the earth on a macroscale, perfect coupling certainly does not occur on the microscale. With the aid of contact mechanical modeling and concepts, it can be shown that this lack of contact at the microscale, or rather the change thereof during a sweep, can have a significant effect on the dynamics of the vibrator-earth system. Modeling of such changing contact predicts that the dynamic behavior varies considerably with the vibrator drive level. The most significant effect predicted by the model is a decrease in the base-plate resonance frequency with an increasing drive level. Extensive drive-level tests carried out in a field experiment confirm this change of resonance behavior with drive level.

INTRODUCTION

Seismic vibrators are typically used to send out sweep signals. Distributing frequency content over time reduces the amount of instantaneous power that a vibrator has to deliver, but these lengthy signals need to be compressed during processing. To do this, one needs to know the source signal, which is most commonly measured at the vibrator.

Measuring the source signal, however, is not a trivial task, because the source consists of multiple elements that dynamically interact with each other. A model of the main components of a vibrator is shown in Figure 1. The most common method to determine the source wavelet is the weighted-sum-ground-force method (Castanet and Lavergne, 1965). This method relies on two basic assumptions: First, it is assumed that the total force a vibrator exerts on the ground can be measured, and second, it is assumed that this force is a measure of the seismic wavelet in the far-field.

The force the vibrator exerts on the ground is determined by summing the measured accelerations of the reaction mass and base plate, after being multiplied with their respective mass. In this way, the net forces on the reaction mass and base plate are added together. From Figure 1, it is clear that the forces between the plate and reaction (RM support and driving force) are removed from this sum. The forces left in the sum are the support of the hold-down mass and the total of the interaction between the base plate and the earth (HD support and BP-earth interaction). Typically, the hold-down mass is ignored because its support is designed to pass its weight without affecting the dynamics of the base plate at frequencies above approximately 5 Hz. Therefore, the weighted sum of the reaction mass and base-plate acceleration equals the total force on the ground (with opposite sign). Although this method is now most common, there was some debate before it was accepted, see papers by Lerwill (1981), Sallas and Weber (1982), Lerwill (1982), and Sallas (1984).

The assumption that the seismic wavelet measured in the far-field is, up to a derivative, proportional to the total force the vibrator exerts on the ground, can be taken from the work of Miller and Pursey (1954, 1955). Miller and Pursey (1954), similar to the earlier work of Reissner (1936), formulate the behavior of an isotropic elastic half-space with a uniform circular pressure field acting on it. They find that, in such a case, the particle displacement is proportional to the pressure. If the pressure beneath the base plate is uniform, it simply equals the force divided by the plate area, and therefore, the seismic wavelet in the far-field should be proportional to the weighted-sum ground force.

However, in practice, there is a difference between the weighted-sum-ground-force signal and the wavelet observed in the far-field. Many papers are devoted to the mismatch among the actual force (typically measured with load cells), the weighted-sum-ground-force method, and the seismic far-field wavelet; see, for example, Baeten et al. (1988), Van Der Veen et al. (1999), Wei (2008, 2009), Shan et al. (2009), Saragiotis et al. (2010), Wei et al. (2010), Sallas (2010), and Poletto et al. (2011). Any difference between the seismic far-field wavelet and the source wavelet measured at, and used

Manuscript received by the Editor 10 May 2015; revised manuscript received 4 November 2015; published online 12 April 2016.
[1]TU-Delft, Delft, Netherlands and Deltares, Utrecht, Netherlands. E-mail: rik.noorlandt@deltares.nl.
[2]TU-Delft, Delft, Netherlands. E-mail: g.g.drijkoningen@tudelft.nl.
© 2016 Society of Exploration Geophysicists. All rights reserved.

Downloaded 08/03/16 to 131.180.58.123. Redistribution subject to SEG license or copyright; see Terms of Use at http://library.seg.org/

to control, the source will cause a decrease of source repeatability and seismic resolution. Martin and Jack (1990), Aritman (2001), and Meunier (2011) provide some examples.

The mismatch is a direct consequence of the assumptions made not being valid. The vibrator components are typically assumed to be rigid, whereas in practice they are not. Baeten and Ziolkowski (1990) propose a model to account for the flexibility of the base plate. In their model, the contribution of the base-plate acceleration to the weighted-sum ground force is adjusted and decreases with frequency. Their model shows that flexure of the base plate is mainly of importance at high frequencies. Lebedev and Beresnev (2005) come to the same conclusion and also show that although the flexure is not influencing the waves radiating from the source much, it does affect the measurement of the base-plate acceleration. In their examples, different positions of the acceleration sensor on the base plate cause traveltime mismatches of up to approximately 0.6 ms.

In addition to the base-plate flexure, the fact that the vibrator is placed on a rough surface (as indicated in Figure 1), also causes the assumption of a uniform pressure distribution beneath the base plate to be violated. Although this will mainly affect the propagation at higher frequencies only, where wavelengths becomes more nearly equal to the size of the base plate (Lebedev and Beresnev, 2005), it can have a major influence on the dynamics of the vibrator, as we will show in this paper.

The contact between the vibrator and the earth as a cause of signal distortion has been mentioned in the past. Lebedev and Beresnev (2004) and Lebedev et al. (2006) propose a model in which the contact acts as a nonlinear spring. In their model, the "contact spring" is weaker in tension (base plate moving away from the contact) than in compression (base plate moving toward the contact). In this paper, this contact behavior is studied in more detail. First, we show some results of quasistatic modeling. The importance of the shape of a contact is made clear by an analytical example. The outcome of numerical modeling of a rough contact and its sensitivity to several parameters are presented. Then, we describe a dynamic model that can not only reproduce the quasistatic results of the rough contact but also is capable of predicting the behavior of the contact when a sweep force is applied to the base plate. The predictions of the dynamic model are then compared with some field measurements. The field measurements were carried out to investigate the nonlinear, drive-level-dependent behavior of the vibroseis setup. We conclude this paper with a discussion of this work, its implications for field surveys and conclusions that may be drawn.

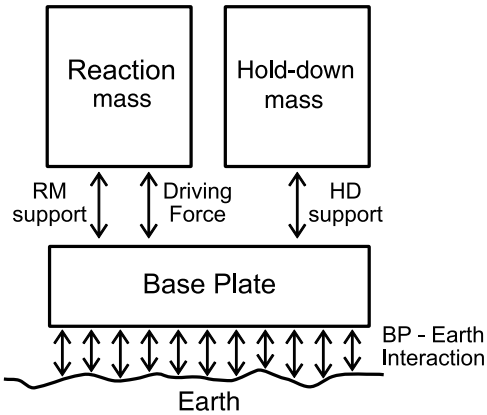

Figure 1. Model of main components of a seismic-exploration vibrator. The driving engine is placed between the reaction mass and base plate (driving force). Parallel to this there might be a support structure to hold the reaction mass (RM support). To prevent the base plate from decoupling from the earth a hold-down system might be present (HD support). The translation of the forces between the elements of the vibrator to a seismic wave occurs at the contact between the base plate and the earth (BP-earth interaction).

CONTACT MECHANICS

Normally, a seismic vibrator is not fixed to the ground, and its contact is simply established by its weight. The driving engine is then used to generate a time-varying pressure that is added to the static pressure caused by gravity. The total pressure can increase and decrease, but care is taken to make sure that some pressure is left to keep the vibrator, at least at macroscale, in contact with the ground. Normally, the (static) gravity component is ignored because it is not recorded by the geophones. However, this can only be done if the vibrator-earth system behaves linearly, which is most probably not the case as indicated by the harmonics observed in the field. The displacement of the ground might not be linearly related to the driving force due to the intrinsic material properties or the geometry of the setup or both. Although material-induced nonlinearity changes from material to material, geometry-induced nonlinearity can in principle occur with every material beneath the vibrator, such as soil, rock, asphalt, concrete, ice, etc. The main goal of this paper is to describe the effect such a contact geometry might have.

Although the vibrator plate is relatively flat, the ground underneath is not. Therefore, at the microscale, the plate will not be in contact with the ground over its complete or nominal area, as shown in Figure 1. In general, the true contact area, places where ground and base-plate molecules interact, is only a fraction of the nominal contact area. Measurements presented by Dean et al. (2015) show that 3% of the contact area can carry as much as 20% of the total load. The distribution of the plate-earth contacts is a function of the applied force and therefore will change under dynamic loading.

The study of the pressure and contact distribution is part of the field of contact mechanics; for a good introduction, see the book of Popov (2010). Hertz (1881) published one of the first papers describing the behavior of two elastic materials in contact. He shows that if two curved elastic half-spaces are pressed together, the displacement and contact area are related in a nonlinear way to the force applied.

Simple contact geometry

The exact force-displacement relation strongly depends on the shape and material of the bodies brought in contact. To illustrate the effect of shape, Figure 2 shows the cross section of differently curved bodies and their force-displacement relations when pressed on a flat half-space of the same material. The shape of these modeled bodies has a vertical axis of symmetry and a height h proportional to the distance to this symmetry axis r raised to a certain power n:

$$h(r) = \alpha^{(1-n)} r^n, \tag{1}$$

where α is a normalization constant. In our example, the value of α was set to 250 mm, equal to maximum value of r. The base of these

Downloaded 08/03/16 to 131.180.58.123. Redistribution subject to SEG license or copyright; see Terms of Use at http://library.seg.org/

shapes becomes flatter with increasing power. The behavior of such axisymmetric contacts has, for example, been described by Heß (2012) and Popov (2013). The force-displacement relation for power law profiles shown in Figure 2a is given by equation 21 of Popov (2013) and is proportional to the applied force to a power $n/(n+1)$ as plotted in Figure 2b. The flatness of the base is clearly reflected in these force-displacement curves. It is clear that the smallest displacement for a given force is produced by two flat surfaces brought into contact. The flatter the contact, i.e., the higher the power used, the better it approaches the linear behavior of two flat bodies brought into contact. For contacts with this geometry, the contact acts as a spring that becomes stiffer (weaker) with increasing (decreasing) force.

Rough surface contact

Although the axisymmetric contact example shows an important property of contact mechanics, it is not well-suited to describe real-life situations for at least two reasons. First, the geometries are assumed to be perfect, and second, there is only a single contact acting. If two real materials are pressed together there typically will be several locations were the two materials are in contact. The number of locations and the shape of these contacts change with the applied load. The calculation of solutions to this problem is not straight forward because "the displacement at any point of the surface depends on the entire pressure distribution inside the contact area (Heß, 2012)" and, in general, numerical schemes solve this iteratively. Typically, a certain total displacement is assumed, and the associated deformation and pressure distributions are calculated. The total of the pressure distribution is then compared with the applied load and the total displacement is adjusted until they match. To investigate the behavior of the vibrator-soil contact, we made use of a program based on Vollebregt (2014), but similar results can be obtained with the code made available by Sainsot and Lubrecht (2011). Both programs are able to quasistatic model the deformation of arbitrary, but discretized, surfaces brought into contact under different loading. In principle, the smallest details of the ground microtopography should be taken into account, but, following the argument of Persson (2001), there typically exists a natural macroscopic limit to the smallest details needed to accurately model the contact behavior.

To obtain an idea of the typical force-displacement curves belonging to the vibrator-ground contact, a sensitivity study was carried out, using varying profile roughness (lateral and vertical) and soil materials. The base plate was modeled as a flat solid steel plate with a constant shear modulus of 80 GPa and a Poisson's ratio of 0.3. The grid that was used to perform the calculation was 1×1.8 m, similar to the size of the base plate of the vibrator used in the field which is described later, and was sampled every 2.2 mm, resulting in a grid of approximately 370,000 height samples. Three different levels of profile coarseness were created with a pseudorandom number generator. The coarsest grid was created by populating 100 samples uniformly over the 370,000 grid points and interpolating in between. For the finer grids 900, respectively, 8100 samples were used as starting point. The grids were filtered to remove wavelengths below 10 mm, as to prevent numerical artifacts in the modeling. Finally, these three grids were cumulatively summed and normalized. Figure 3 shows an example of the three grids produced in this way.

Figure 4a shows the force-displacement relation when the steel base plate is pushed onto the different profiles presented in Figure 3, assuming a ground shear modulus of 100 MPa, a Poisson's ratio of 0.45, and a maximal profile height of 1 mm. For comparison, the result obtained with a flat profile has been plotted as well. The force range was chosen roughly the same as that of a typical vibrator with a static hold-down force of approximately 300 kN and a driving force of approximately ±275 kN. The results of the rough contact profiles differ significantly from that of the flat contact, but are mutually hardly distinguishable. Using the profile in Figure 3c, the height, shear modulus, and Poisson's ratio were varied to study their impact on the force-displacement curves. These results are shown in Figure 4b–4d, respectively.

From the curves in Figure 4, it is clear that the force-displacement relation shows a different behavior at small and large loads. At small loads, the curve is nonlinear and similar to the force-displacements

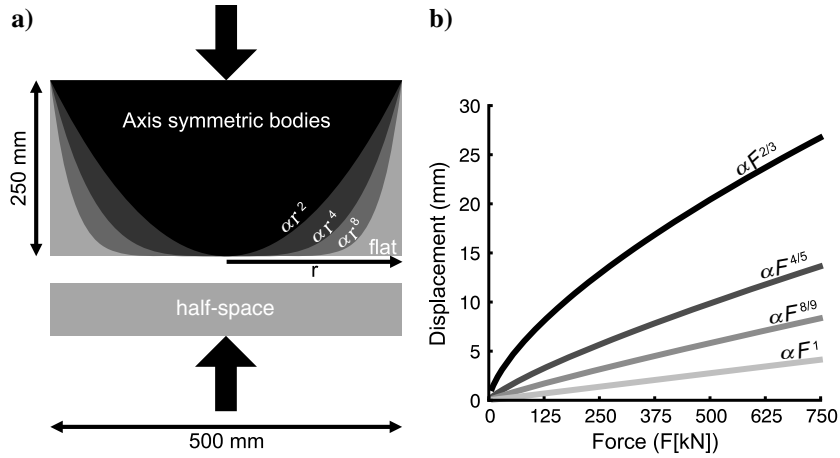

Figure 2. The 3D axis symmetric bodies. (a) Different gray scales and (b) their force-displacement relation when pressed onto a half-space of the same material. The black arrows indicate the direction of the force and displacement. Values for parameters: shear modulus: 200 MPa; Poisson's ratio of 0.45.

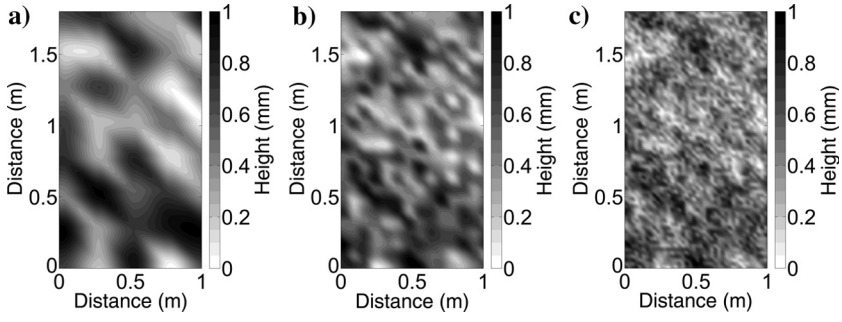

Figure 3. Profiles as used to model the force-displacement relations. Increasing lateral details from (a-c).

Downloaded 08/03/16 to 131.180.58.123. Redistribution subject to SEG license or copyright; see Terms of Use at http://library.seg.org/

shown in Figure 2; the contact becomes stiffer with force. At larger loads, the curves shown in Figure 4 deviate from those in Figure 2 by showing almost linear behavior. The reason for this dual behavior is simple. At small loads, only a limited number of contacts are actively carrying the load. With an increasing load, the area of contact expands rapidly, until, at high loads, this expansion rate decreases and the contact starts to behave more and more as one single flat contact, leading to a more linear behavior. This is also the reason why profile height and strength play a dominant role because they control how easily the profile becomes "flat" under loading. The different profiles and Poisson's ratios did not affect the force-displacement relation significantly. Because the modeling relies on the pseudorandom number generator, the calculation was repeated for 20 different starting seeds. These calculations produced very similar force-displacement relations.

It is important to note that the loads in Figure 4 represent total load, i.e., the sum of the static and dynamic forces of the vibrator. It shows that in those parts of a sweep in which the dynamic force on the base-plate points in the downward direction, i.e., increasing the total load, the contact behaves more linear. However, if the dynamic force drives the base plate upwards, the contact becomes less linear. At high drive levels, the total load can decrease significantly during parts of the sweep, and although the vibrator stays in contact with the ground, the relative resistance it experiences from the ground is greatly reduced. In that sense, base-plate decoupling should be considered as a gradual process, instead of a binary one. Also note that, comparing these results with the contact models of Lebedev et al. (2006), the rest position and load of the vibrator does not act as special situation from which behavior is different in a compression or tension state. In the examples given in Figure 4, a transition between behaviors occurs at forces that only depended on the geometry and parameters of the contact itself.

The curves shown in Figure 4 are only valid for elastic interaction, such that the profiles recover their original shapes, when they are not in contact anymore. The ground-vibrator interaction, however, causes permanent deformation, mainly to the ground, as well. When the base plate is lowered and the hold-down system is activated, the pressure on the individual contact points can easily exceed the elastic limit. The soil will deform until both surface profiles are more alike and the pressure is shared by a larger contact area. During a sweep, the pressure on the ground dynamically reaches (much) larger values, and as long as the contact area is not large enough to sustain the local pressure elastically, permanent deformation will occur. It is expected that the role of permanent deformation will decrease after several sweeps, such that the elastic behavior, with a force-displacement relation similar to that of Figure 4, but with a fixed permanent displacement offset, becomes dominant. Although the role of permanent deformation is expected to decrease with the number of sweeps, it will not always be the case. Meunier (2011, p. 112, figure 20) provides an example, in which even after 60 sweeps the difference between the 59th and 60th record, amplified by a factor of 20, resembles the 59th record. This clearly indicates that conditions between the 59th and 60th varied and most probably were caused by permanent deformation of the road on which the vibrator was placed.

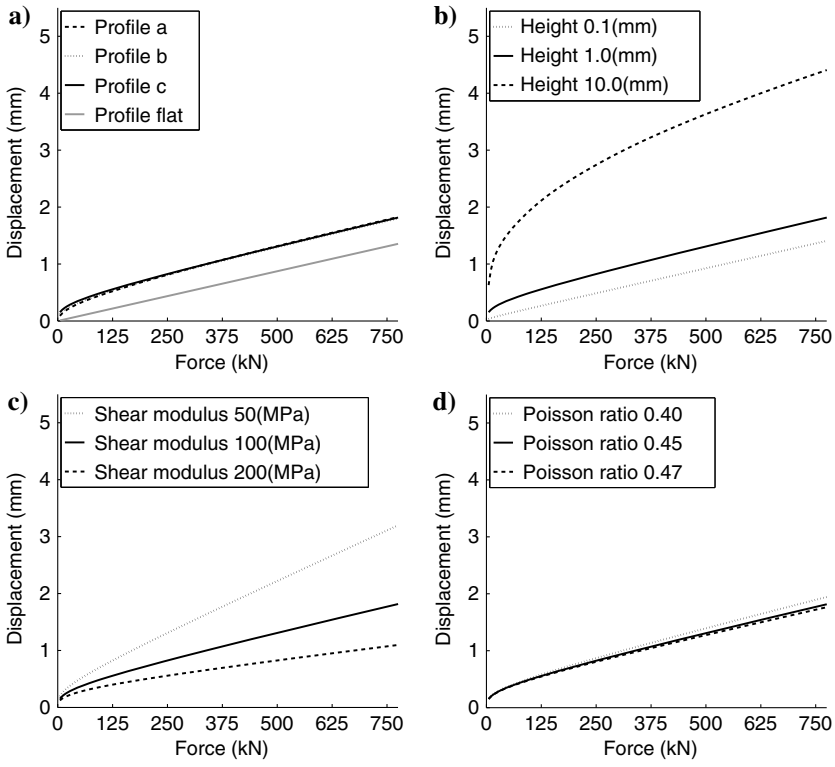

Figure 4. Force-displacements curves for (a) the different profiles of Figure 3 (also including flat soil surface response), (b) different maximum profile heights, (c) different shear moduli, and (d) Poisson's ratios. The solid black curve is repeated in all plots and represents a reference: profile (c) with a maximum height of 1 mm, a shear modulus of 100 MPa, and a Poisson's ratio of 0.45.

Contact dynamics: Single nonlinear spring

Knowing the force-displacement relation of a quasistatic contact, it is instructive to investigate the dynamic effect such a relation would have on the base plate. Because our main interest is the effect of the contact, we ignored the dynamic behavior of the reaction mass and hold-down system, but did take into account their weight on the top of the base plate. The contact spring (beneath the base plate) was chosen to behave such as the reference contact (solid black curve of Figure 4). This setup has some similarities with a Duffing oscillator (Walker, 1995). Analytic solutions for such systems can only be found under some very restrictive conditions, mainly due to the fact that the solutions strongly depend on the driving amplitude and damping. Therefore, we chose to model the time behavior numerically, using a standard ordinary differential equation (ODE) solver. The driving force was a simple 12 s 8–80 Hz linear sweep, with 250 ms cosine tapers on both ends, the same was used for the field measurements described later. Some damping was needed to prevent the base plate from decoupling. The amount of damping was set such that at 100% drive level, the dynamic forces on the base plate just did not exceed the static ones.

Figure 5 shows a small time window of the modeled acceleration of the base plate for differ-

Downloaded 08/03/16 to 131.180.58.123. Redistribution subject to SEG license or copyright; see Terms of Use at http://library.seg.org/

ent drive levels. At low drive levels, the signal stays sinusoidal, but at high drive levels, the acceleration amplitude becomes asymmetric and more sawtooth shaped. It is clear that even for a linear elastic earth, the contact between the vibrator and soil can cause a nonlinear distortion on the base-plate acceleration and therefore will affect the weighted-sum-ground-force signal.

Contact dynamics: Winkler foundation

Up to now, we have used the quasistatic approach to determine the contact behavior. Although this gives useful insights, a crucial property of the contact dynamics might have been ignored. Consider the potential vibrator-ground contact area to be divided in three groups: part of the area will stay in contact at all times, part of that area will never get in direct contact, and in some area the contact will be made and lost repeatedly during the sweep. The behavior of this last group is not well-represented in the examples above nor in the model proposed by Lebedev and Beresnev (2004) and might give a twist to the quasistatic results presented before, because this group might behave dynamically on their own while not in contact with the vibrator.

To solve the rough contact problem dynamically in a fully 3D setup is difficult and there is hardly any literature available on this topic. For these kinds of problems, the difficult 3D problem is typically replaced by a phenomenological model that is much simpler, but captures the essence of the problem. Instead of the contact, a set of linear springs with different heights, also called a Winkler foundation, is modeled. Rules for converting the full problem to such a model can be found in the work done by Heß (2012) and Popov (2013). Lebedev and Beresnev (2004), based on the work of Rudenko and Vu (1994), propose to use a Winkler foundation model (Figure 1 in their paper) to describe the vibrator-earth contact. To analyze the dynamic behavior of the contact, we use a similar model, see Figure 6, with the difference that the contact springs (top springs in Figure 6) are not allowed to extend beyond a certain threshold value (different for each spring) and are connected to some "ground" mass. Each individual ground mass is allowed to move freely but has a restoring force with respect to its displacement from a certain reference plane. In this model, the ground can move independently from the base plate, making the dynamic behavior most likely different from its static behavior.

Instead of trying to convert our rough profiles shown in Figure 3 to an equivalent Winkler foundation directly, we chose to use the quasistatic results (Figure 4), modeled with the program from Vollebregt (2014), and fit these with the multispring model of Figure 6. The force-displacement curves obtained with rough surfaces, presented in Figure 4, indicate that the contact becomes stiffer with increasing load. For the multispring model, this translates to more springs being in contact with the base plate at higher loads. Two steps were made to determine the appropriate spring height distribution, and hence the number of springs in contact at a certain displacement, to fit the reference force-displacement relation of Figure 4. First, the spring constants were fixed to a fraction of the smallest stiffness found in the force-displacement curve. Second, the number of springs needed to compensate the load was calculated at every displacement along the curve. For the reference curve in Figure 4, approximately 50 springs were needed. As a last step, the masses between the springs were chosen such that their sum equaled the mass of the base plate.

With these parameters, the behavior of the base plate was then determined numerically when loaded with a static force of approximately 320 kN and driven by a linear sweep at many different drive levels ranging from 10% to 90% of 275 kN. Some damping was added to the masses to keep the base plate in contact to at least a single mass-spring unit.

It is interesting to study the resulting transfers from the driving force, the linear sweep, to the base-plate displacement for different drive levels. Figure 7 shows the amplitude and phase response of the system when driven by a linear 8–80 Hz 12 s sweep. For this contact model, the base plate has a resonance frequency of approximately 60 Hz at the 10% drive level, which interestingly drops down to approximately 44 Hz at the 90% drive level. If the system is described as a single harmonic oscillator, the resonance frequency would be proportional to the square root of the effective stiffness.

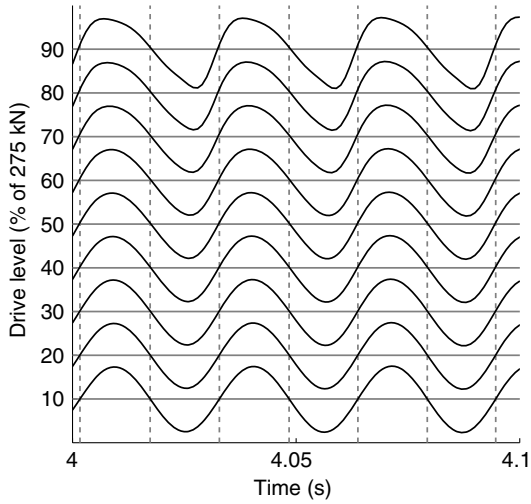

Figure 5. Small time window of the modeled base-plate acceleration when driven by a 12 s linear sweep from 8 to 80 Hz and placed on a contact spring with a force-displacement shown by the solid black line in Figure 4. Amplitudes were normalized for drive level.

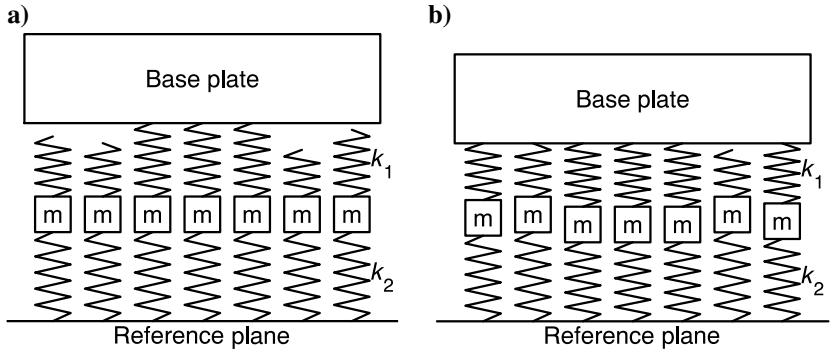

Figure 6. Multispring contact model. (a) Base plate just before it exerts a force on the ground, only a few springs are in contact. (b) After applying the static load of the weight of the base plate, reaction and hold-down mass, more springs are in contact and some masses are displaced.

Downloaded 08/03/16 to 131.180.58.123. Redistribution subject to SEG license or copyright; see Terms of Use at http://library.seg.org/

A frequency drop of approximately 75% thus translates to a reduction of the effective stiffness by almost a half. The amplitude and the width of the frequency peak increases slightly from low drive level to higher. Some striped patterns below the resonance frequency and especially at large force levels, indicating harmonic distortion, are also visible.

FIELD OBSERVATIONS

In 2012, a data set was obtained specifically focused on determining the amplitude-dependent behavior of vibrator-soil interaction. Part of the data shown here were presented before by Noorlandt et al. (2013). The experiment took place near Devine, Texas. The vibrator used was a modified 266 kN (60,000 lbf) vibrator from INOVA, mounted on an AHV-IV vehicle. The modifications mainly dealt with reducing the harmonic distortion. The experiment basically consisted of repeating the same linear 8–80 Hz 12 s sweep, with different drive levels. Ten different drive levels from 5% to 90% were used, and each drive level was repeated 10 times. After finishing the last sweep at a drive level of 90%, the whole sequence was repeated. In total, 200 sweeps were performed without moving the vibrator or lifting the base plate. The entire experiment was repeated at a second location only 20 m from the first, but with different top soil conditions. At the first location, the base plate was placed on grass-covered soil, at the second location on bare soil. The vibrator controller was set to follow the amplitude of weighted-sum ground force and the phase of the reaction mass. This was done such that the vibrator stayed within safe limits, without incorporating too much phase information from the base plate.

The idea behind this procedure is to get information on the influence of the drive level, permanent deformation, and repeatability of the source. Permanent deformation is thought to be dependent mainly on the soil characteristics directly beneath the base plate, the maximum amount of force applied, and the number of sweeps. By keeping the vibrator on the same location during the experiment, it is expected that the compaction of the soil reduces with number of sweeps performed. It is thus expected that the last sweeps of each set of 10 are more comparable than the first, and that after completing the first sequence, the lower drive-level sweeps of the second sequence are more repeatable than those of the first sequence.

Figure 8 shows the measured accelerations and weighted-sum-ground-force amplitude spectra for the first location. In that figure, each force strip consists of 10 consecutive sweeps. The figure displays a total of 200 sweeps. The amplitudes have been divided by drive-level percentages to make them comparable. Several observations can be made. First of all, it is clear that the controller does a good job, especially above approximately 24 Hz; the weighted-sum-ground-force signal has a flat amplitude spectrum, whereas the individual acceleration signals have not. The 10 sweeps done at each drive level produce very comparable amplitude spectra and the repeatability in both sequences seems to be equal. The most striking, however, is that the base-plate acceleration signals show a resonance, whose frequency decreases with the drive level. In the second sequence, the amplitude of the base-plate resonance is a little bit smaller at the lower drive levels.

To study this behavior in more detail, a correction has to be made for the fact that the driving signal was adjusted dynamically by the controller and thus has no flat spectra, as is clearly shown in Figure 8a. To remove the effect of the controller, the dynamic transfer from the total driving force acting on the base plate to its displacement was calculated. Ignoring the hold-down system again,

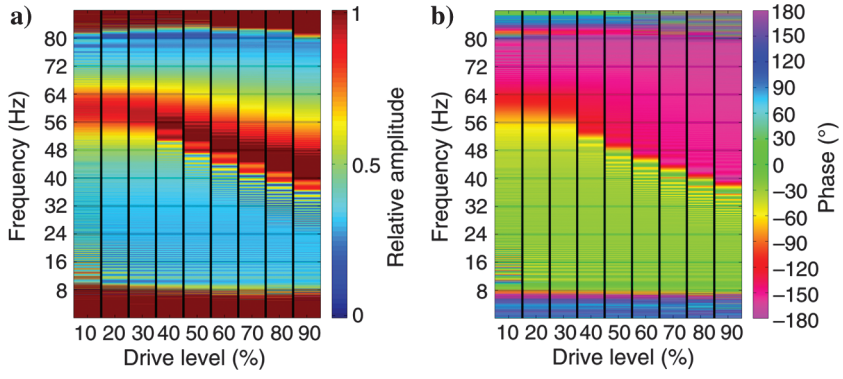

Figure 7. Transfer of driving force to base-plate displacement for multispring contact model (Figure 6). (a) Amplitude and (b) phase spectra for different drive levels.

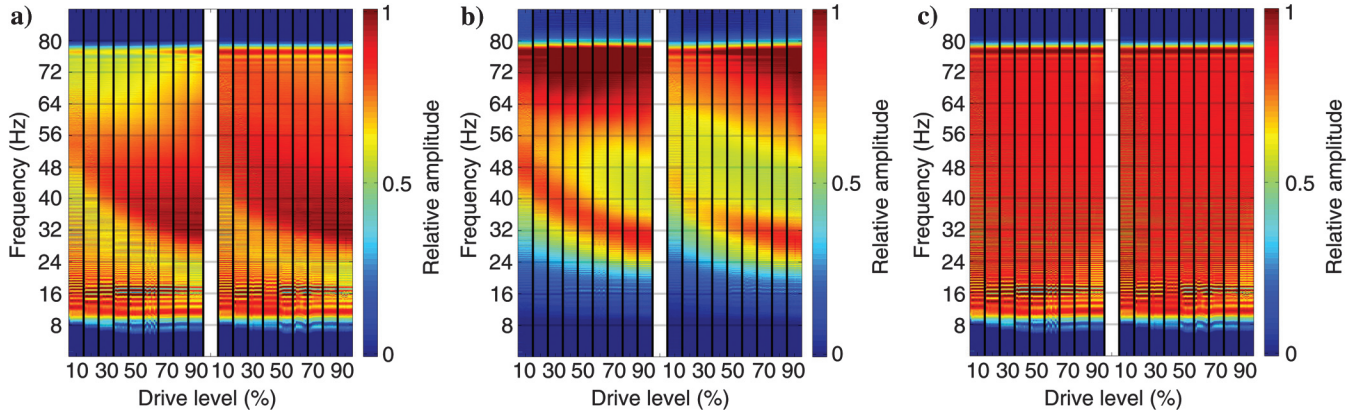

Figure 8. Measured amplitude spectra for different drive levels at first location (grass-covered soil). (a) Reaction mass, (b) base-plate acceleration, and (c) the weighted-sum combination of both. Amplitudes divided by drive-level percentages.

Downloaded 08/03/16 to 131.180.58.123. Redistribution subject to SEG license or copyright; see Terms of Use at http://library.seg.org/

the total driving force equals the reaction mass times its (negative) acceleration (Figure 1). The base-plate displacement can be found by twice integrating its acceleration, which was done in the frequency domain. Having determined both signals, the transfer function is obtained by dividing the displacement signal by the force signal.

Figure 9 shows the transfer functions obtained for the first location, whereas Figure 10 shows the transfers for the second location nearby. The responses at these locations differ a bit, but the main features coincide. In both cases, a resonance is present that becomes stronger with the drive level. Also the frequency at which this amplification occurs decreases with the drive level; although, this is clearer in the first location and sequence than in the second location. Comparing the first sequence with the second sequence, it is notable that the behavior at the low drive levels is less comparable between sequences than those of the high drive levels. This is probably caused by the permanent deformation of the ground beneath the vibrator due to the high force levels in the first sequence. Furthermore, at the second location, where the vibrator was placed on bare soil, dust clouds from underneath the base plate were observed at high frequencies. The amount of dust did not noticeably decrease, even for the very last sweep, indicating that the contact was relatively poor and still reshaping even after approximately 200 sweeps.

Besides the dynamic aspects of the vibrator, the wavelet that the vibrator produces at different drive levels is, from a seismic perspective, even more interesting. Figure 11 shows for the first location the measured weighted-sum ground force and geophone response at 850 m depth after correlation with the pilot signal. The ground-force signal is almost completely the same for all drive levels and the two different sequences. It is also symmetric in time, indicating that the pilot and weighted-sum ground force are very alike. However, the signal measured in the borehole is not as stable and changes with drive level. The first arrival shifts a couple of ms to later times when comparing the 5% and the 90% case, for both sequences. The recordings of both sequences are very similar, indicating that the difference in spectra between these sequences (Figures 8 and 9) only have minor effect. Similar time shifts with drive-level variation were observed by Martin and Jack (1990). Therefore, it should be stressed that the weighted-sum-ground-force signal is only an estimate of the vibrator signature, and depending on soil conditions and drive level, might be less applicable. Similar observations were presented by Meunier (2011, p. 109, figure 16).

DISCUSSION

There are quite some similarities between the measured transfer signals shown in Figures 9 and 10 and the modeled transfers of the Winkler foundation model shown in Figure 7. In both cases, a resonance frequency is present whose frequency decreases with amplitude. Such shift of frequency cannot be predicted by a fully linear model in which source amplitude does not play a role in the dynamic behavior. It is therefore tempting to interpret the frequency shifts observed in the field as a contact-mechanical effect; however, the vibrator-earth contact might not be the only effect observed.

Reust (1993) argues that, because most soils are sublinear (force-weakening), a decrease of resonance frequency with increasing drive level could be expected (see his figure 5). In a field experiment comparable to ours, Johnson et al. (2009) find very similar decreases of resonance frequency with drive level. They contribute this frequency decrease to "modulus softening as a function of drive amplitude" and show that this happens both at the source and between the (nearby) receivers (see their figures 7 and 8). Their argument to calculate the receiver-receiver ratios is to "reduce any contamination from potential nonlinear coupling of the vibrator plate to the ground." Because the resonance behavior in their source-to-receiver ratios is different from their receiver-to-receiver ratios, we conclude that contact mechanics played a role in their measurements.

It would be nice to be able to distinguish material and contact induced nonlinearity, but for this, further investigation of this topic is needed. Below, we discuss several shortcomings and improvement possible to the modeling, experiment, and processing.

Several simplifications were made in the modeling. All of the results in this work are based on the assumption that the materials

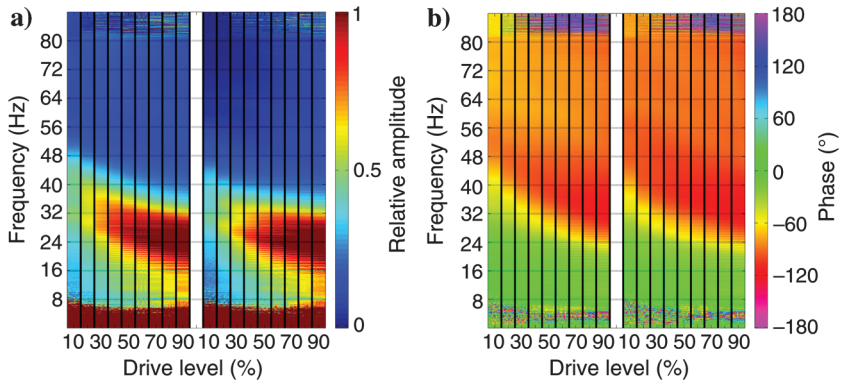

Figure 9. Transfer of total driving force to base-plate displacement for field data at first location (grass-covered soil). (a) Amplitude and (b) phase spectra for two sequences of increasing drive levels.

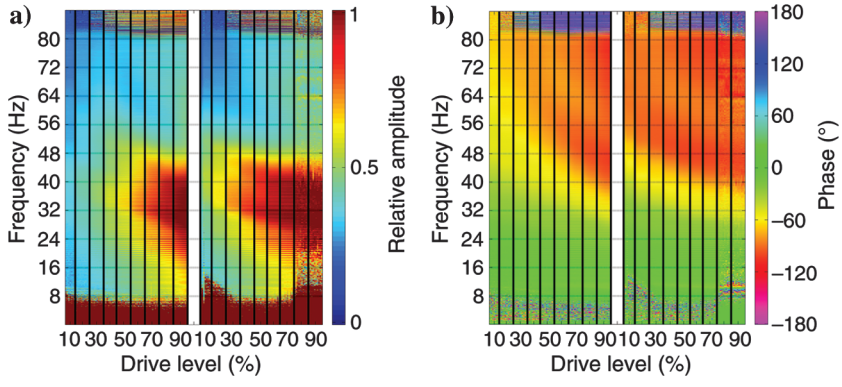

Figure 10. Transfer of total driving force to base-plate displacement for field data at second location (bare soil, 20 m away from first location). (a) Amplitude and (b) phase spectra for two sequences of increasing drive levels.

Downloaded 08/03/16 to 131.180.58.123. Redistribution subject to SEG license or copyright; see Terms of Use at http://library.seg.org/

in contact can be described as linear elastic continua, which might not be appropriate for the materials a seismic vibrator encounters in the field, such as rock, soil, asphalt, concrete, etc. From the often observed permanent deformation of the material below the base plate, it is clear that this material does not behave purely elastically or, as the work of Johnson et al. (2009) indicates, linear. In our approach to use the quasistatic results in the multispring model (Figure 6), the horizontal interaction within the contact was ignored completely. This should be taken into account because a vertical pressure will convert to vertical and horizontal displacements and thus will lead to a different deformation of the contact area than the one predicted by the current model.

On the experiment side, the main shortcoming is that only two vibrator parameters are measured, such as the accelerations of the base plate and reaction mass. Converting these two macroscopic parameters to many microscopic parameters is inherently nonunique. Load cells or more accelerometers will not solve this problem because first of all they provide macroscopic information only, and second, in the case of load cells, they alter the contact dramatically. However, insight in the dynamics of the vibrator-ground contact can be obtained with a pressure mapping device, without affecting the contact a lot. Results presented by Dean et al. (2015) are promising and show that the pressure underneath the base plate is far from uniform.

Regarding the data processing, one could argue that the concept of a transfer function is only valid in the linear regime and care has to be taken not to over interpret the results for the nonlinear case observed. Some of the response might be more dependent on timing, and thus on the choice of sweep, than on frequency as suggested by the plot. To be able to determine the time dependency, not only the amplitude of the sweep should be changed but also its frequency range and sweep rate.

Implications for field measurements

Several lessons can be drawn from the conducted studies. From the modeling conducted it is clear that the contact behaves most nonlinear at small total loads (Figure 4). To avoid small total loads, the dynamic force on the base plate should be substantially smaller than the static force given by the total weight of the base plate, reaction mass, and hold-down system. Although not directly confirmed by our field data, lower drive levels did produce smaller levels of resonance amplification. Preparation of the contact can help to minimize the contact-mechanical effects. The smaller the height of the airs gaps between the base plate and the earth the better (Figure 4b). To decrease the influence of permanent deformation insweeping seems to be a good idea, but from the field measurements it is observed that this is probably only effective if the contact preparation sweeps have a (much) larger drive level than the succeeding (production) sweeps. Measuring the pressure distribution underneath the complete base plate with a thin sensor would capture the effect of the base-plate flexure and contact mechanical effects, leading to a better ground force estimation. The work of Dean et al. (2015) showed that this is now possible.

CONCLUSION

We show that the contact between the vibrator and ground can have a significant effect on the behavior of the vibrator. Even if the applied force on the ground stays within its linear elastic limits, the geometry of the vibrator-ground contact can cause the displacement to respond nonlinearly to the applied force. As a consequence, the displacement changes asymmetrically with a force increase or decrease. Extending the quasistatic force-displacement relation to a dynamic study, with the help of a Winkler foundation model, it was shown that a reduction in base-plate resonance frequency with

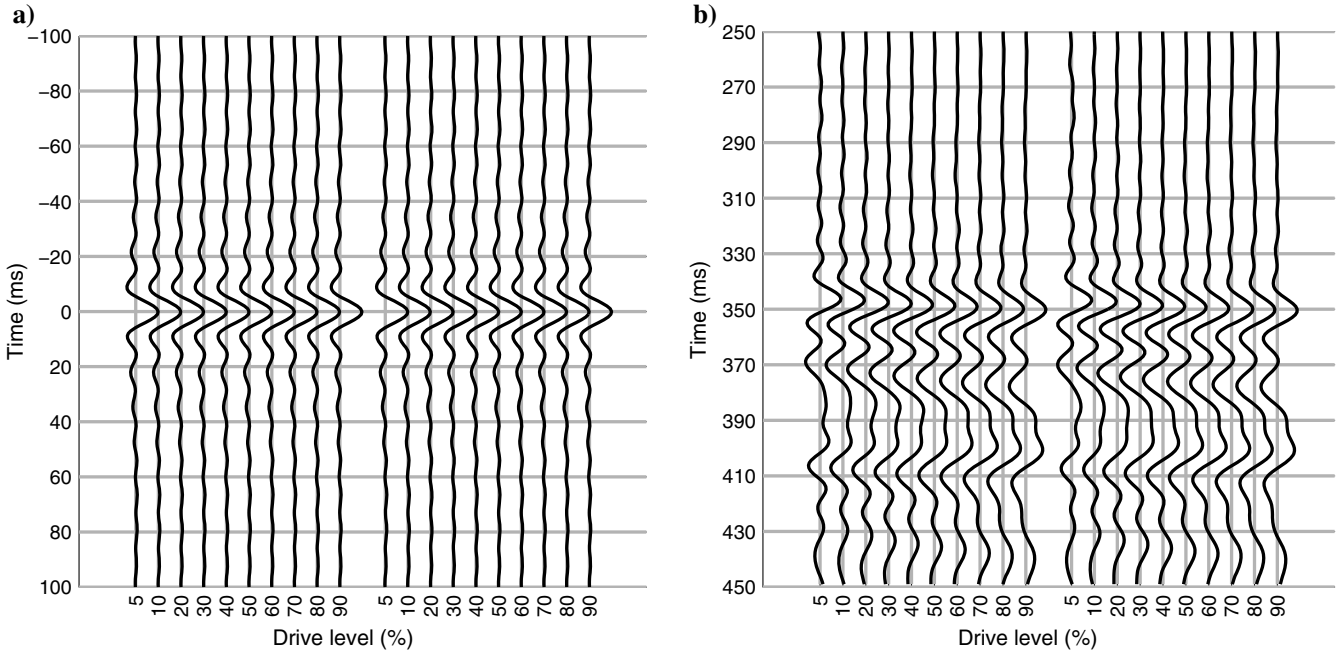

Figure 11. (a) Weighted-sum ground-force signal and (b) vertical-component borehole-geophone signal correlated by normed pilot signal for different drive levels. For each drive level, the eighth sweep was plotted. Amplitudes divided by drive-level percentages and normed by overall maximum per plot.

the drive level was to be expected. Field measurements performed with different drive levels show similar behavior, but other causes cannot be excluded and have been discussed. Moreover, the field measurements showed that the measured weighted-sum ground force was stable for different drive levels, but that the shape and timing of the wavelet observed in the borehole was not. Overall, it should be concluded that the drive level, next to the kind of sweep, is an important control variable.

ACKNOWLEDGMENTS

We are grateful that ION together with INOVA Geophysical offered us the possibility to perform the field experiments and allowed us to present these data. We would especially like to thank K. Faber for his contributions to the fieldwork. We would also like to thank Shell for funding these experiments. This work has been sponsored by the Research School of Integrated Earth Sciences (ISES). It is also supported by the Nederlandsche Aardolie Maatschappij (NAM) and Deltares. We would like to thank the six reviewers for their constructive comments and suggestions.

REFERENCES

Aritman, B. C., 2001, Repeatability study of seismic source signatures: Geophysics, **66**, 1811–1817, doi: 10.1190/1.1487123.

Baeten, G., and F. Strijbos, 1988, Wave field of a vibrator on a layered half-space: Theory and practice: 58th Annual International Meeting, SEG, Expanded Abstracts, 92–96.

Baeten, G., and A. Ziolkowski, 1990, The vibroseis source: Elsevier.

Castanet, A., and M. Lavergne, 1965, Vibrator controlling system: U.S. Patent 3,208,550.

Dean, T., P. Vermeer, M. Laycock, J. Tulett, and D. Lane, 2015, The complexity of vibrator baseplate-ground interaction measured with a thin-film pressure pad and a downhole tool: 77th Annual International Conference and Exhibition, EAGE, Extended Abstracts, We P6 07.

Hertz, H., 1882, Ueber die berührung fester elastischer körper: Journal für die reine und angewandte mathematik, **92**, 156–171.

Heß, M., 2012, On the reduction method of dimensionality: The exact mapping of axisymmetric contact problems with and without adhesion: Physical Mesomechanics, **15**, 264–269, doi: 10.1134/S1029959912030034.

Johnson, P. A., P. Bodin, J. Gomberg, F. Pearce, Z. Lawrence, and F.-Y. Menq, 2009, Inducing in situ, nonlinear soil response applying an active source: Journal of Geophysical Research: Solid Earth, **114**, B05304, doi: 10.1029/2008JA014017.

Lebedev, A., and I. Beresnev, 2004, Nonlinear distortion of signals radiated by vibroseis sources: Geophysics, **69**, 968–977, doi: 10.1190/1.1778240.

Lebedev, A., and I. Beresnev, 2005, Radiation from flexural vibrations of the baseplate and their effect on the accuracy of traveltime measurements: Geophysical Prospecting, **53**, 543–555, doi: 10.1111/j.1365-2478.2005.00492.x.

Lebedev, A., I. Beresnev, and P. Vermeer, 2006, Model parameters of the nonlinear stiffness of the vibrator-ground contact determined by inversion of vibrator accelerometer data: Geophysics, **71**, no. 3, H25–H32, doi: 10.1190/1.2196870.

Lerwill, W., 1981, The amplitude and phase response of a seismic vibrator: Geophysical Prospecting, **29**, 503–528, doi: 10.1111/j.1365-2478.1981.tb00691.x.

Lerwill, W., 1982, Reply to comments by Sallas and Weber on "the amplitude and phase response of a seismic vibrator": Geophysical Prospecting, **30**, 939–941, doi: 10.1111/j.1365-2478.1982.tb01349.x.

Martin, J., and I. Jack, 1990, The behaviour of a seismic vibrator using different phase control methods and drive levels: First Break, **8**, 404–414, doi: 10.3997/1365-2397.1990022.

Meunier, J., 2011, Seismic acquisition from yesterday to tomorrow: 2011 distinguished instructor short course: SEG.

Miller, G., and H. Pursey, 1954, The field and radiation impedance of mechanical radiators on the free surface of a semi-infinite isotropic solid: Proceedings of the Royal Society of London. Series A, Mathematical and Physical Sciences, **223**, 521–541, doi: 10.1098/rspa.1954.0134.

Miller, G., and H. Pursey, 1955, On the partition of energy between elastic waves in a semi-infinite solid: Proceedings of the Royal Society of London. Series A. Mathematical and Physical Sciences, **233**, 55–69, doi: 10.1098/rspa.1955.0245.

Noorlandt, R., G. Drijkoningen, and C. Faber, 2013, Influence of drive level on the fundamental vibrator signal: 75th Annual International Conference and Exhibition incorporating SPE EUROPEC 2013, EAGE, Extended Abstracts, Th P11 02.

Persson, B. N., 2001, Theory of rubber friction and contact mechanics: The Journal of Chemical Physics, **115**, 3840–3861, doi: 10.1063/1.1388626.

Poletto, F., A. Schleifer, F. Zgauc, and L. Petronio, 2011, Borehole signals obtained using surface seismic sources and ground-force sensors: 81st Annual International Meeting, SEG, Expanded Abstracts, 4298–4303.

Popov, V. L., 2010, Contact mechanics and friction: Springer.

Popov, V. L., 2013, Method of reduction of dimensionality in contact and friction mechanics: A linkage between micro and macro scales: Friction, **1**, 41–62, doi: 10.1007/s40544-013-0005-3.

Reissner, E., 1936, Stationäre, axialsymmetrische, durch eine schüttelnde Masse erregte Schwingungen eines homogenen elastischen Halbraumes: Archive of Applied Mechanics, **7**, 381–396.

Reust, D. K., 1993, Enhanced servovalve technology for seismic vibrators: Geophysical Prospecting, **41**, 43–60, doi: 10.1111/j.1365-2478.1993.tb00564.x.

Rudenko, O., and C. Vu, 1994, Nonlinear acoustic properties of a rough surface contact and acousto diagnostics of a roughness height distribution: Acoustical Physics, **40**, 668–672.

Sainsot, P., and A. Lubrecht, 2011, Efficient solution of the dry contact of rough surfaces: A comparison of fast Fourier transform and multigrid methods: Proceedings of the Institution of Mechanical Engineers, Part J: Journal of Engineering Tribology, **225**, 441–448, doi: 10.1177/1350650111401535.

Sallas, J., 1984, Seismic vibrator control and the downgoing P-wave: Geophysics, **49**, 732–740, doi: 10.1190/1.1441701.

Sallas, J., 2010, How do hydraulic vibrators work? A look inside the black box: Geophysical Prospecting, **58**, 3–18, doi: 10.1111/j.1365-2478.2009.00837.x.

Sallas, J., and R. Weber, 1982, Comments on "the amplitude and phase response of a seismic vibrator" by W. E. Lerwill: Geophysical Prospecting, **30**, 935–938, doi: 10.1111/j.1365-2478.1982.tb01348.x.

Saragiotis, C., P. Scholtz, and C. Bagaini, 2010, On the accuracy of the ground force estimated in vibroseis acquisition: Geophysical Prospecting, **58**, 69–80, doi: 10.1111/j.1365-2478.2009.00851.x.

Shan, S., P. M. Eick, J. D. Brewer, X. Zhu, and S. A. Shaw, 2009, Load cell system test experience: Measuring the vibrator ground force on land seismic acquisition: 79th Annual International Meeting, SEG, Expanded Abstracts, 16–20.

Van Der Veen, M., J. Brouwer, and K. Helbig, 1999, Weighted sum method for calculating ground force: An evaluation by using a portable vibrator system: Geophysical Prospecting, **47**, 251–267, doi: 10.1046/j.1365-2478.1999.00133.x.

Vollebregt, E. A., 2014, A new solver for the elastic normal contact problem using conjugate gradients, deflation, and an FFT-based preconditioner: Journal of Computational Physics, **257**, 333–351, doi: 10.1016/j.jcp.2013.10.005.

Walker, D., 1995, Harmonic resonance structure and chaotic dynamics in the earth-vibrator system: Geophysical Prospecting, **43**, 487–507, doi: 10.1111/j.1365-2478.1995.tb00263.x.

Wei, Z., 2008, Design of a P-wave seismic vibrator with advanced performance: GeoArabia, **13**, 123–136.

Wei, Z., 2009, How good is the weighted-sum estimate of the vibrator ground force?: The Leading Edge, **28**, 960–965, doi: 10.1190/1.3192844.

Wei, Z., M. Hall, and T. Phillips, 2010, Optimizing the weighted-sum signal to represent the actual force output from the vibrator: 72nd Annual International Conference and Exhibition, EAGE, Extended Abstracts, P291.

Downloaded 08/03/16 to 131.180.58.123. Redistribution subject to SEG license or copyright; see Terms of Use at http://library.seg.org/